Supplemental Figures

Figure S1

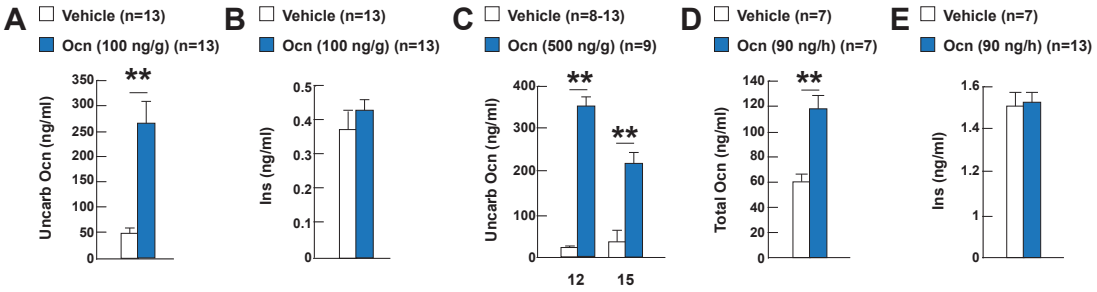

Figure S2

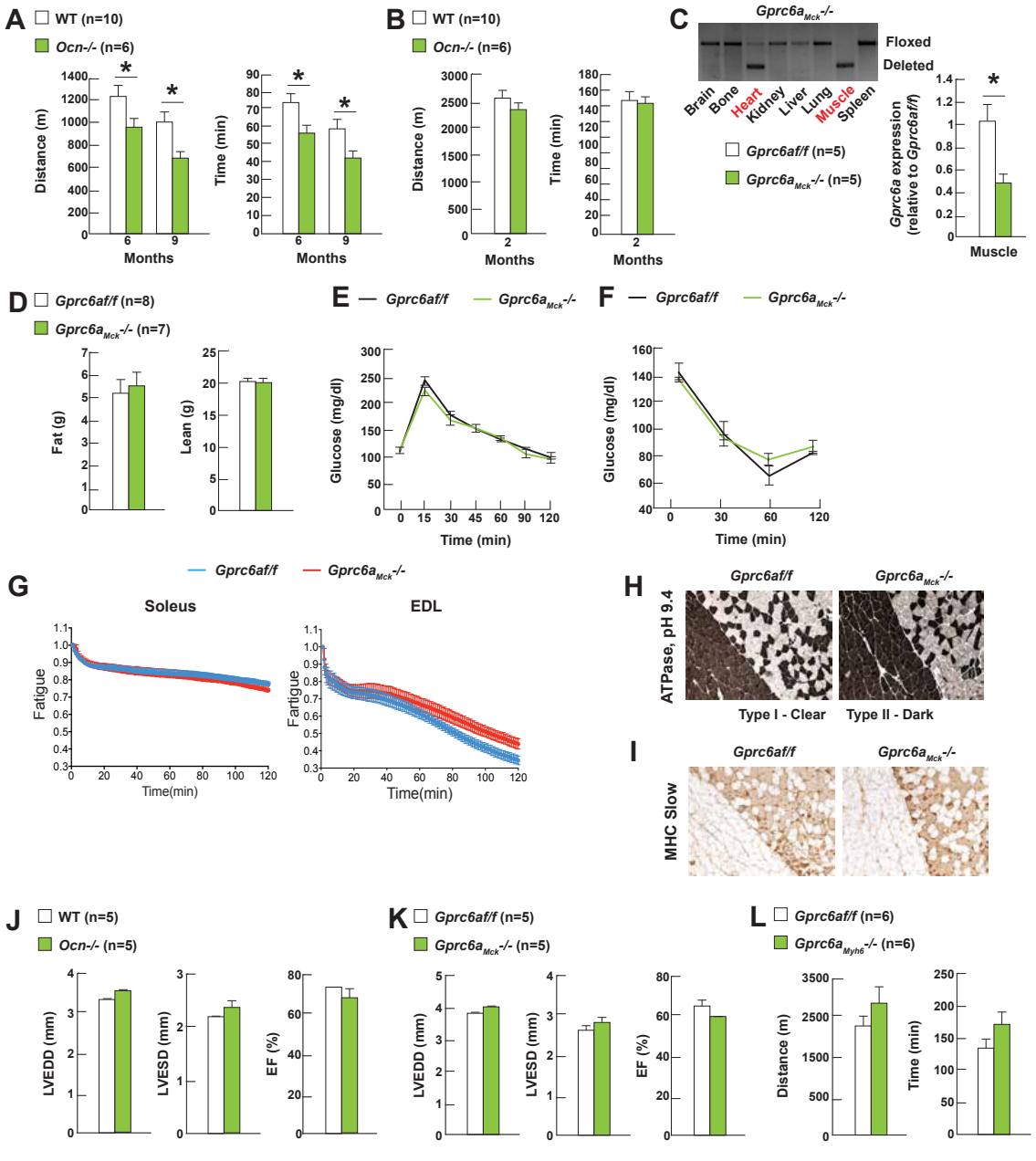
A
WT (n=10)
Ocn-/- (n=6)
Distance (m)
Time (min)
Months
B
WT (n=10)
Ocn-/- (n=6)
Distance (m)
Time (min)
Months
C
Gprc6a Mck-/-
Floxed
Deleted
Brain
Bone
Heart
Kidney
Liver
Lung
Muscle
Spleen
Gprc6af/f (n=5)
Gprc6a Mck-/- (n=5)
Gprc6a expression (relative to Gprc6af/f)
Muscle
D
Gprc6af/f (n=8)
Gprc6a Mck-/- (n=7)
Fat (g)
Lean (g)
E
Gprc6af/f
Gprc6a Mck-/-
Glucose (mg/dl)
Time (min)
F
Gprc6af/f
Gprc6a Mck-/-
Glucose (mg/dl)
Time (min)
G
Gprc6af/f
Gprc6a Mck-/-
Soleus
EDL
Fatigue
Time(min)
H
Gprc6af/f
Gprc6a Mck-/-
ATPase, pH 9.4
Type I - Clear
Type II - Dark
I
Gprc6af/f
Gprc6a Mck-/-
MHC Slow
J
WT (n=5)
Ocn-/- (n=5)
LVEDD (mm)
LVESD (mm)
EF (%)
K
Gprc6af/f (n=5)
Gprc6a Mck-/- (n=5)
LVEDD (mm)
LVESD (mm)
EF (%)
L
Gprc6af/f (n=6)
Gprc6a Myh6-/- (n=6)
Distance (m)
Time (min)

Figure S3

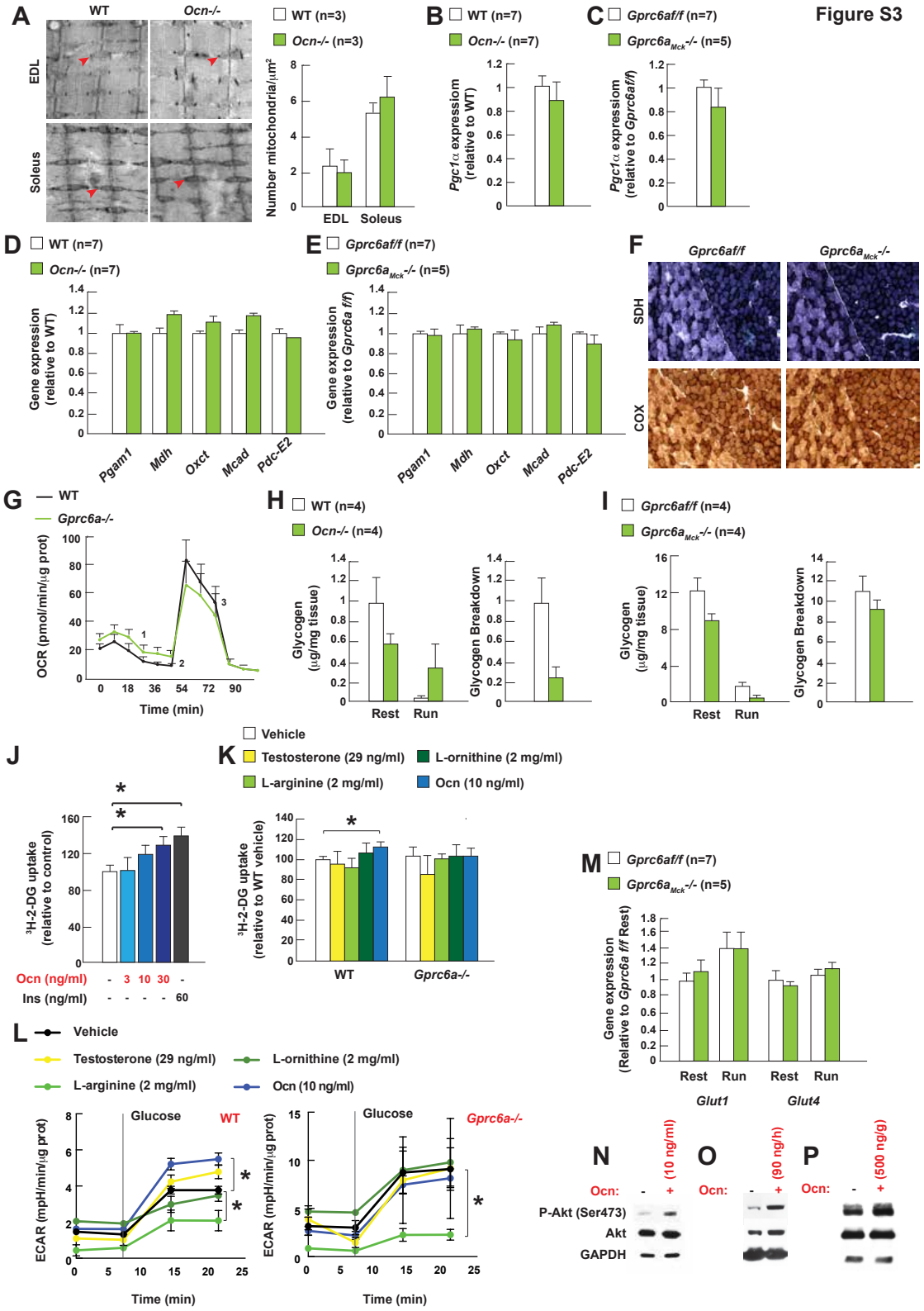
A
WT
Ocn-/-
EDL
Soleus
WT (n=3)
Ocn-/- (n=3)
Number mitochondria/μm²
EDL
Soleus
B
WT (n=7)
Ocn-/- (n=7)
Pgc1α expression (relative to WT)
C
Gprc6af/f (n=7)
Gprc6aMck-/- (n=5)
Pgc1α expression (relative to Gprc6af/f)
D
WT (n=7)
Ocn-/- (n=7)
Gene expression (relative to WT)
Pgam1
Mdh
Oxct
Mcad
Pdc-E2
E
Gprc6af/f (n=7)
Gprc6aMck-/- (n=5)
Gene expression (relative to Gprc6a f/f)
F
Gprc6af/f
Gprc6aMck-/-
SDH
COX
G
WT
Gprc6a-/-
OCR (pmol/min/μg prot)
Time (min)
H
WT (n=4)
Ocn-/- (n=4)
Glycogen (μg/mg tissue)
Glycogen Breakdown
Rest
Run
I
Gprc6af/f (n=4)
Gprc6aMck-/- (n=4)
J
3H-2-DG uptake (relative to control)
Ocn (ng/ml)
Ins (ng/ml)
K
Vehicle
Testosterone (29 ng/ml)
L-ornithine (2 mg/ml)
L-arginine (2 mg/ml)
Ocn (10 ng/ml)
3H-2-DG uptake (relative to WT vehicle)
WT
Gprc6a-/-
L
Vehicle
Testosterone (29 ng/ml)
L-ornithine (2 mg/ml)
L-arginine (2 mg/ml)
Ocn (10 ng/ml)
Glucose
WT
Gprc6a-/-
ECAR (mpH/min/μg prot)
Time (min)
M
Gprc6af/f (n=7)
Gprc6aMck-/- (n=5)
Gene expression (Relative to Gprc6a f/f Rest)
Rest
Run
Glut1
Glut4
N
Ocn:
(10 ng/ml)
P-Akt (Ser473)
Akt
GAPDH
O
Ocn:
(90 ng/h)
P
Ocn:
(500 ng/g)

Figure S4

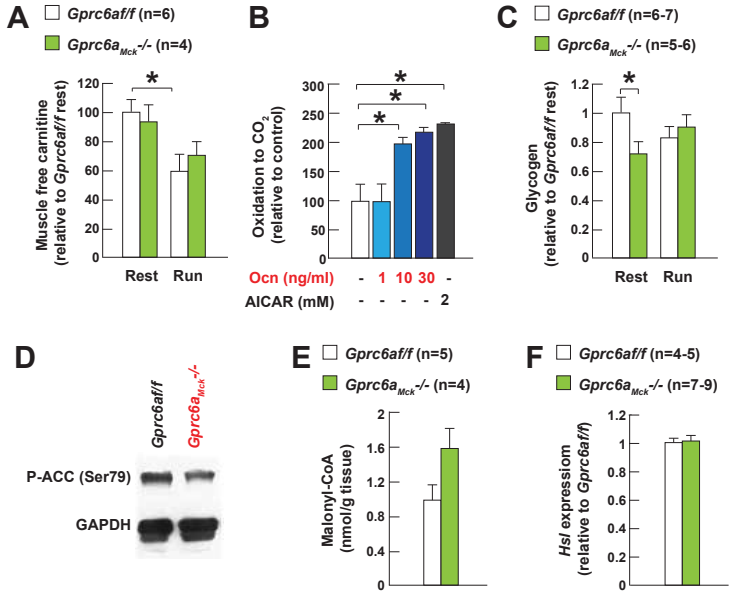
A
Gprc6af/f (n=6)
Gprc6a$_{Mck}$-/- (n=4)
Muscle free carnitine (relative to Gprc6af/f rest)
120
100
80
60
40
20
0
*
Rest
Run
B
Oxidation to CO$_2$ (relative to control)
300
250
200
150
100
50
0
*
*
*
Ocn (ng/ml) - 1 10 30 -
AICAR (mM) - - - - 2
C
Gprc6af/f (n=6-7)
Gprc6a$_{Mck}$-/- (n=5-6)
Glycogen (relative to Gprc6af/f rest)
1.2
1
0.8
0.6
0.4
0.2
0
*
Rest
Run
D
Gprc6af/f
Gprc6a$_{Mck}$-/-
P-ACC (Ser79)
GAPDH
E
Gprc6af/f (n=5)
Gprc6a$_{Mck}$-/- (n=4)
Malonyl-CoA (nmol/g tissue)
2
1.6
1.2
0.8
0.4
0
F
Gprc6af/f (n=4-5)
Gprc6a$_{Mck}$-/- (n=7-9)
Hsl expressiom (relative to Gprc6af/f)
1.2
1
0.8
0.6
0.4
0.2
0

Figure S5

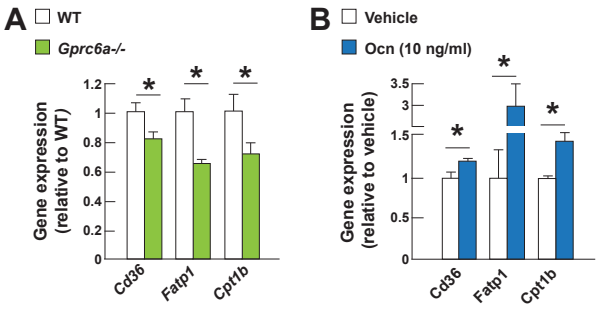
A
WT
Gprc6a-/-
Gene expression (relative to WT)
1.2
1
0.8
0.6
0.4
0.2
0
*
*
*
Cd36
Fatp1
Cpt1b
B
Vehicle
Ocn (10 ng/ml)
Gene expression (relative to vehicle)
3.5
3
1.5
1
0.5
0
*
*
*
Cd36
Fatp1
Cpt1b

Figure S6


A
Gprc6a f/f
Gprc6a Mck -/-
1 2 3 4 5 1 2 3 4
Il6
Mstn
Bdnf
Il1r1
Dcn
Fam132b
Fndc5
Il15
B
Vehicle (n=5)
IL-6 (3 ng/g) (n=4)
IL-6 (pg/ml)
18
16
14
12
10
8
6
4
2
0
Ocn-/-

Supplemental Figure Legends

Figure S1. Related to Figure 1. Regulation of circulating osteocalcin levels by exercise and age.

A. Serum undercarboxylated osteocalcin (uncarb Ocn) levels in 3 month-old WT mice injected with vehicle or Ocn immediately before running.

B. Serum insulin (Ins) levels in 3 month-old WT mice injected with vehicle or Ocn immediately before running.

C. Serum uncarb Ocn levels in 12 and 15 month-old WT mice injected with vehicle or Ocn immediately before running.

D. Serum total Ocn and **E**. Ins levels in 10 month-old WT mice treated with Ocn for 28 days.

Figure S2. Related to Figure 2. Osteocalcin signaling in myofibers is necessary for adaptation to exercise.

A. Performance during an endurance test (running on a treadmill at 30cm/s until exhausted) of 6 and 9 month-old *Ocn-/-* and WT mice and **B**. 2 month-old *Ocn-/-* and WT mice.

C. PCR analyses of *Gprc6a* deletion in various tissues in *Gprc6a*$_{Mck}$*-/-* mice and qPCR analyses of *Gprc6a* expression in gastrocnemius muscle of *Gprc6a*$_{Mck}$*-/-* and control mice.

D. Body composition in 3 month-old *Gprc6a*$_{Mck}$*-/-* and *Gprc6af/f* mice.

E. GTT in 3 month-old *Gprc6a*$_{Mck}$*-/-* and *Gprc6af/f* mice.

F. ITT in 3 month-old *Gprc6a$_{Mck}$-/-* and *Gprc6af/f* mice.

G. Muscle contraction and resistance to fatigue in isolated soleus and EDL muscles of *Gprc6a$_{Mck}$-/-* and *Gprc6af/f* mice.

H. ATPase staining in gastrocnemius/soleus muscle of 3 month-old *Gprc6a$_{Mck}$-/-* and *Gprc6af/f* mice.

I. Myosin heavy chain (MHC) slow staining in gastrocnemius/soleus muscle of 3 month-old *Gprc6a$_{Mck}$-/-* and *Gprc6af/f* mice.

J. Heart function of 3 month-old *Ocn-/-* and WT mice and **K**. *Gprc6a$_{Mck}$-/-* and *Gprc6af/f* mice measured by echocardiograpy.

L. Performance during an endurance test (running on a treadmill at 30cm/s until exhausted) of 3 month-old *Gprc6af/f* and *Gprc6a$_{Myh6}$-/-* mice.

Figure S3. Related to Figure 3. Osteocalcin signaling in myofibers promotes uptake and utilization of glucose during exercise.

A. Mitochondria number in EDL and soleus of 3 month-old WT and *Ocn-/-* mice measured by electronic microscopy.

B. *Pgc1α* expression in *Ocn-/-* and WT mice and **C**. *Gprc6af/f* and *Gprc6a$_{Mck}$-/-* mice after exercise.

D. *Pgam1, Mdh, Oxct, Mcad and Pdc-E2* expression in *Ocn-/-* and WT and **E**. *Gprc6af/f* and *Gprc6a$_{Mck}$-/-* mice after exercise.

F. SDH and COX activities in gastrocnemius/soleus muscles of *Gprc6af/f* and *Gprc6a$_{Mck}$-/-* mice after exercise.

G. Mitochondrial respiration measured in *Gprc6a-/-* and WT myofibers after the addition of (1) oligomycing, (2) FCCP and (3) rotenone.

H. Glycogen content and breakdown in 3 month-old WT and *Ocn-/-* tibialis muscles at rest and after exercise.

I. Glycogen content and breakdown in 3 month-old *Gprc6af/f* and *Gprc6a*$_{Mck}$*-/-* liver at rest and after exercise.

J. Uptake of ^{3}H-2-deoxyglucose (^{3}H-2-DG) in WT myotubes treated with vehicle or osteocalcin (Ocn).

K. Uptake of ^{3}H-2-deoxyglucose (^{3}H-2-DG) in WT and *Gprc6a-/-* myotubes treated with vehicle, testosterone, L-arginine, L-ornithine or Ocn.

L. Glycolysis determined by the extracellular acidification of the media (ECAR), in WT and *Gprc6a-/-* myofibers treated with vehicle testosterone, L-arginine, L-ornithine or Ocn.

M. *Glut1* and *Glut4* expression in *Gprc6af/f* and *Gprc6a*$_{Mck}$*-/-* in gastrocnemius muscle at rest and after exercise.

N. Western blot analyses of Akt phosphorylation (Ser473) in WT myotubes treated with Ocn.

O. Western blot analyses after exercise of Akt phosphorylation (Ser473) in tibialis muscles of 3 month-old WT mice injected with Ocn and **P**. in tibialis muscles of 15 month-old WT mice injected with Ocn.

(Exercise refers to 40 min running at 30cm/s on a treadmill).

Figure S4. Related to Figure 4. Osteocalcin signaling in myofibers favors FAs utilization during exercise.

A. Free carnitine levels in quadriceps muscles of 3 month-old *Gprc6af/f* and *Gprc6a$_{Mck}$-/-* mice at rest and after exercise.

B. ^{14}C-Oleate oxidation in WT myotubes treated with vehicle, osteocalcin (Ocn) or AICAR as a positive control.

C. Plasma NEFAs levels in *Gprc6af/f* and *Gprc6a$_{Mck}$-/-* mice at rest and after exercise.

D. Western blot analyses after exercise of ACC phosphorylation (Ser79) in tibialis muscles of 3 month-old *Gprc6af/f* and *Gprc6a$_{Mck}$-/-* mice.

E. Malonyl-CoA levels in quadriceps muscles of 3 month-old *Gprc6af/f* and *Gprc6a$_{Mck}$-/-* mice after exercise.

F. Expression of *Hsl* in gastrocnemius muscles of 3 month-old *Gprc6af/f* and *Gprc6a$_{Mck}$-/-* mice after exercise.

(Exercise refers to 40 min running at 30cm/s on a treadmill).

Figure S5. Related to Figure 5. Osteocalcin signaling in myofibers favors expression of FAs transporters during exercise.

A. *Cd36*, *Fatp1* and *Cpt1b* expression in WT and Gprc6a-/- myotubes and **B**. WT myotubes treated with vehicle or Ocn.

Figure S6. Related to Figure 6. Osteocalcin is necessary for the increase in *Interleukin-6* expression in muscle during exercise.

A. Expression of myokines in gastrocnemius muscles of 3 month-old *Gprc6af/f* and *Gprc6a*$_{Mck}$*-/-* mice after exercise.

B. Plasma IL-6 levels in 3 month-old *Ocn-/-* mice injected with vehicle or IL-6 immediately before running.

Supplemental Experimental Procedures

Monkeys and human studies

Healthy volunteers were used to assay osteocalcin (Elecsys, Roche Diagnosis) across lifespan. For children aged 10-18, age, body mass index (kg/m^2) and Tanner's stages were recorded. Children with past or present therapy with growth hormone, corticosteroids (more than 3 months), or any chronic diseases were excluded. Adult individuals were selected using the following criteria: normal body mass index, no history of smoking, fracture, diabetes, chronic diseases and anti-osteoporotic agent usage. Young adult women were non menopausal and not pregnant. Studies were approved by local ethic comity of Lyon University, France. Comparison between groups was performed using Mann-Whitney non-parametric tests and trend was assessed using logistic regression.

Rhesus monkeys (*Macaca mulatta*) were housed at the NIH Animal Center, Poolesville, MD. Monkeys were housed individually in standard non-human primate caging on a 12h light/12h dark cycle, room temperature 78 ± 2 degrees humidity at 60 ± 20%. All monkeys had extensive visual, auditory, and olfactory but limited tactile contact with monkeys housed in the same room. Monkeys received 2 meals per day *ad libitum*. Water was always available *ad libitum*. Monkeys were anesthetized with either Ketamine, 7-10 mg/kg, IM or Telazol, 3-5 mg/kg, IM. Blood samples were obtained by venipuncture of the femoral vein using a vacutainer and vacuum tubes. Serum was collected and stored at -80 degrees C until assayed.

Ex vivo glucose uptake

Ex vivo glucose uptake in EDL and soleus muscle was measured previously described (Bruning et al., 1998), with two main modifications: first, ^{3}H-2-deoxyglucose (^{3}H-2DG, 1.5 μCi/ml) but not ^{14}C-mannitol, was used. Second, EDL and soleus muscles were processed as follows to separate ^{3}H-2DG and ^{3}H-2DG-6-phosphate. EDL and soleus muscles were homogenized in 500 μl water and boiled for 10 min immediately after. After that, homogenates were spin at max speed for 10 min. 50 μl of the supernatant were added to 450 μl of water and counted in 5 ml of scintillation liquid. 400 μl were passed through an anion exchange column (AG 1-X8 resin, Bio-Rad) to remove ^{3}H-2DG-6-phosphate. Column was washed with 2 ml of water and 500 μl of the eluted volume were counted in 5 ml of scintillation liquid. The difference between the total and eluted ^{3}H radioactivity represents ^{3}H-2DG-6-phosphate accumulated in the tissue.

In vivo glucose uptake

For in vivo glucose uptake, a modification of a previously described method (Howlett et al., 2013) was used with some modifications. An initial pilot experiment with a group of WT resting and WT exercising mice was performed to validate the method. Briefly, mice were injected prior to exercise with 10 μCi of ^{3}H-2-deoxyglucose (^{3}H-2DG) in 100 μl of 0.9% NaCl. Next, mice were placed on a treadmill and were forced to run for 40 min at a constant speed (30cm/s). After exercise, blood glucose and quadriceps muscles were collected to determine ^{3}H radioactivity. ^{3}H radioactivity in blood was similar in all mice, indicating similar systemic delivery of the tracer. To determine ^{3}H-2DG-6-phosphate accumulation in the tissue, muscles were processed as follows: white and red quadriceps

muscles were homogenized in 1 ml of water and boiled for 10 min immediately after. After that, homogenates were spin at max speed for 10 min. 50 μl of the supernatant were added to 450 μl of water and counted in 5 ml of scintillation liquid. 900 μl were passed through an anion exchange column (AG 1-X8 resin, Bio-Rad) to remove ^{3}H-2DG-6-phosphate. Column was washed with 6 ml of water and 500 μl of the eluted volume were counted in 5 ml of scintillation liquid. The difference between the total and eluted ^{3}H radioactivity represents ^{3}H-2DG-6-phosphate accumulated in the tissue.

Transfection of C2C12 myoblasts for analyses of GLUT4 translocation

The day before transfection, C2C12 myoblasts were plated in 6-well plates (100,000 cells/well). Cells were co-transfected with HA-glut4-gfp and Gprc6a-myc plasmids using Lipofectaine 2000® (Invitrogen) at a ratio 1:4 (μg DNA:μl Lipofectamine 2000®) in combination with 2 μl of CombiMag™ (OZBiosciences) magnetic nanoparticles in Opti-MEM™ (Invitrogen) media. Cells were incubated with the mix for 30 min on a magnetic plate at room temperature. 8 h after transfection, cells were cultured in complete growth media (DMEM high glucose, 10% FBS, 1% penicillin/streptomycin). 24 h after transfection cells were used for the analyses of GLUT4 translocation as previously described (Zeigerer et al., 2002).

Energy metabolism in myofibers

For energy metabolism studies myofibers were isolated from flexor digitorum brevis muscle and used in all experiments after an overnight incubation in

matrigel-coated plates with DMEM high glucose containing penicillin/streptomycin, gentamycin, pyruvate and 2% FBS. For mitochondrial function studies, the Seahorse XF Cell Mito Stress Test Kit was used following manufacturer's protocol. To determine glucose or FAs utilization, myofibers were incubated in a non-CO_2 incubator for 4 h in KHRB containing exclusively glucose (25 mM) or oleic acid (3 mM) following by the measurement of oxygen consumption rates (OCR). To determine glycolysis, myofibers were cultured in DMEM high glucose containing penicillin/streptomycin, gentamycin, pyruvate but no FBS, for 4 hours. After that, myofibers were treated with vehicle, osteocalcin or other Gprc6a ligands for 1 hour. After treatment, myofibers were incubated with Seahorse XF Assay Medium containing 1 mM glutamine and vehicle, osteocalcin or other Gprc6a ligands for 1 hour in a non-CO_2 incubator and then ECAR was measured before and after the addition of glucose.

Metabolite Profiling

Liquid Chromatography/Mass Spectrometry (LC/MS). Plasma samples were processed using module 1, and tissue samples using module 1 and module 3, at the Einstein Stable Isotope and Metabolomics Core Facility (see http://www.einstein.yu.edu/research/shared-facilities/stable-isotope-metabolomics-core/services/).

Module 1 employs a targeted metabolomics approach using the Absolute IDQ p180 kit (BIOCRATES Life Sciences AG, Innsbruck, Austria) that has proved useful in predicting disorders in fuel homeostasis (Krug et al., 2012; Wang-Sattler et al., 2012). The kit allows simultaneous quantification of 40 acylcarnitines, 90

glycerophospholipids (lysophosphatidylcholine and phosphatidylcholine) and 15 sphingolipids by Flow Injection analysis-Mass Spectrometry (FIA-MS/MS) and 21 amino acids and 20 amino acid metabolites/biogenic amines by LC/MS. The settings follow the manufacturer's instruction for UPLC-MS/MS using the Aquity UPLC and the Xevo TQ MS (Waters, Pittsburgh, PA, USA).

Module 3 employs LC/MS/MS (Waters Xevo TQ). Analysis was used for quantitation of glycolytic, pentose and TCA cycle metabolites as per (Serasinghe et al., 2015). For glycolytic, pentose, and TCA metabolites, chromatographic analysis prior to targeted, multiple reaction monitoring (MRM) mass spectrometric analyses, was performed using an Aquity UPLC using a Waters BEH amide 1.7 µm column 2.1 x 100 mm, and an acidic mobile phase containing an acetonitrile/water gradient, as per (Serasinghe et al., 2015). Samples were bracketed in between calibration standards and linear regression was performed for quantitation.

LC/MS sample preparation. For plasma samples using module 1, 10 µl was spotted per well and processed as per kit instructions. For the skeletal muscle samples, the same extract was used for both modules 1 and 3. Approximately 50 mg of tissue was used per assays. The tissue samples were homogenized with 7 times volume of methanol (with 5mmol ammonium acetate) for the sample weight. 2 µg of internal standard ($U^{13}C$-succinate) was added to each sample prior to homogenization, after which samples frozen in liquid nitrogen were thawed on ice, sonicated and again freeze thawed. The supernatant was used for analysis.

Gas Chromatograph-Time of Flight Mass Spectrometry (GC-TOF MS) sample preparation. The samples were homogenized using10 fold volume to the weight of skeletal muscle tissue, with methanol containing (3 internal standards, 25μM of $U^{13}C$-citrate, 15μM of $U^{13}C$ succinate and 150μM of heptadecanoic acid). After addition of methanol to muscle sample, the sample was homogenized, then an equal volume water was added, homogenized again, frozen in liquid nitrogen, thawed on ice, sonicated and again freeze thawed, The supernatant was used for analysis. After lyophilization, the samples were methoximized with 50 µl of methoxyamine hydrochloride (MOA, 15 mg/mL in pyridine) at 30 ^{0}C for 90 min. The silylation step was done with 50 µl of N,O-Bis(trimethylsilyl) trifluoroacetamide (BSTFA, containing 1% TMCS) at 70 ^{0}C for 60 min, as per (Qiu et al., 2014).

GC-TOF MS Analysis. The samples were analyzed using a Water GC-TOFMS Premier (Waters, USA) in electron impact ionization (EI) mode. The samples were injected at 270^{0}C with a split ratio of 10. Metabolites separation was performed on a 30-meter DB-5MS column coupled with 10-meter guard column (Agilent, USA). The initial oven temperature was set to 60 ^{0}C and kept for 1 min, then rise to 320 ^{0}C at a rate of 10 ^{0}C/min and kept for 3 min. Helium was used as carrier gas at a consistent flow rate of 1ml/min. The transfer line and the source temperature were set at 250 ^{0}C and 220^{0}C, separately.

Data Analysis. A pooled quality control (QC) sample, comprised of equal amounts from all samples, was injected every 10 samples, regardless of MS method, and the multiple QC injections were used to calculate the coefficient of

variation (CV = standard deviation/mean) for each metabolite. Metabolites having CVs greater than 30% were not considered accurate enough for consideration, and also 75% of all measured sample concentrations for the metabolite should be above the limit of detection (LOD). To select candidate biomarkers, principal component analysis (PCA) and Partial Least Squares Discriminant Analysis (PLS-DA) were used.

^{13}C-glucose tracer studies

The contribution of glucose oxidative metabolism was assessed using mass spectrometry and ^{13}C stable isotope tracer technology. The fractional contributions to the CAC, amino acids and lactate were assayed in muscle homogenates using methods as previously described (Kombu et al., 2011; Zhang et al., 2015). This approach enables isotopically labeled metabolites to be measured with a high degree of sensitivity, following a bolus of $^{13}C_6$ glucose tracer.

GC-MS assays. Following homogenization and centrifugation, the supernatant fractions were decanted and reserved for measurements of concentrations and [^{13}C]label of acetyl-CoA enrichment. The tissue pellets were further extracted using a mixture of acetonitrile and 2-propanol (3:1), centrifuged and then analyzed for CAC, amino acids and related intermediates. Extracts were then dried by nitrogen gas for 1-2 hours and chemically derivatized using MTBSTFA + 1% TBDMCS reagent (N-methyl-N-(tert-butyldimethylsilyl) trifluoroacetamide + 1% tert-butyldimetheylchlorosilane, Regis Technologies, Inc. Morton Grove, IL, USA) at reacted at 70 °C for 30 min. The derivatized products were measured

under Agilent 6890 Gas-Chromatography and Agilent 5973 Mass Spectrometry (GC-MS). A DB-17 MS capillary column (30m × 0.25mm × 0.25 μm) was used in all analysis. The starting oven temperature was set to 80 °C, the pressure was 14.82 psi, and the flow velocity was 45cm/sec. Temperature was then increased to linearly to 220 °C and held for 1 min. The mass spectrometer was in electron-impact (EI), sim mode. CAC and related intermediates, succinate (m/z= 289), fumarate (m/z =287), malate (m/z =419), citrate (m/z=459) were measured. Other intermediates and amino acids, including 3-hydroxyglutarate (m/z= 433), aspartate (m/z =418), glutamate (m/z =432), glutamine (m/z =431) and GABA (m/z =274) were also measured.

The plasma glucose enrichment was measured using a GC-MS method. Briefly, the plasma glucoses were dried and incubated with 100 μl of pyridine:acetic anhydride (2:3) at 75 °C for 30 min. An Agilent 6890 GC system were used to determine the selective ion (Ammonia chemical ionization; CI) m/z 408-414.

*LC-MS assays***.** Acetyl-CoA and succinyl-CoA in muscle was measured by LC-MS methods. Briefly, the supernatant fraction was loaded onto a Supelco solid-phase extraction cartridge ([2-(pyridyl)-ethyl functionalized silica gel] preconditioned with 3 ml of methanol and then added 3 ml of buffer A (1:1 methanol-H_2O with 2% acetic acid). The cartridge was then washed with 3 ml of buffer A to elute impurities, followed sequentially by 3 ml of buffer B (1:1 methanol-H_2O with 50 mM ammonium formate), 3 ml of buffer C (3:1 methanol-H_2O with 50 mM ammonium formate), and 3 ml of methanol to elute the acyl-CoAs. The eluent was evaporated under nitrogen.

The LC was coupled with an API4000 Qtrap Mass Spectormeter (Applied Biosystems, Foster City, CA) operated under positive ionization. Acetyl-CoA was m easured at the 14.2 min elution time and the ions 810/303 – 812/305 were monitored.

Calculations

Fractional contributions of [$^{13}C_6$]glucose to oxidaitve metabolism.The fractional isotopic enrichments (via ^{13}C label incorporation) for each of the intermediates were defined as molar percent enrichment (MPE), after background correction. The MPEs (unit: percent) is calculated as

$$MPE_{(M+n)} = 100 \times \frac{A_i}{\sum_{i=0}^{n} A_i}$$

Where $MPE_{(M+n)}$ is the *n* th ^{13}C labeled mass isotopomer enrichment of the metabolite. *A* is the abundance (arbitrary unit) measured by GC-MS. The variable *i* varied from zero to *n*, while *n* is no more than 6. $A_{(0)}$ is the abundance non-labeled metabolite, and $A_{(i)}$ is the abundance for mass isotopomer labeled with i ^{13}C, regardless of position.

The M+2 (M2) MPE of each of the intermediates reflected the contribution of [$^{13}C_6$]glucose to that intermediate pool. For the measurements of the contribution of [$^{13}C_6$]glucose to oxidative metabolism, the assumption was that the first turn of the CAC produces mostly M+2 [^{13}C]labeled intermediates from [1,2-^{13}C]acetyl-CoA via pyruvate dehydrogenase complex (PDH). Thus, the first turn of the CAC (as measured by M+2 for each intermediates) reflected oxidative metabolism.

Concentrations of intermediates in tissue. The concentrations of the endogenous tissue metabolites were determined by standard curves for each metabolite and the known amount internal standard added to the sample. For the absolute concentrations of fumarate, malate and succinate, internal standards of [$^{13}C_4$] succinate, or (*RS*)-3-hydroxy-[$^{2}H_4$]glutarate were used; glutamine and glutamate concentrations were calculated using [$^{2}H_5$]glutamate or [$^{2}H_5$] glutamine; the acetyl-CoA and succinyl-CoA concentrations were assayed using an internal standard of [$^{2}H_9$]pentanoyl-CoA.

Muscle contractility

Contractile measurements were performed on fast twitch muscle EDL and slow twitch muscle Soleus. Both muscles were dissected from hind limbs and placed in chilled Krebs solution (in mM: 119 NaCl, 4.7 KCl, 2.5 CaCl2, 1.2 KH2PO4, 1.2 MgSO4, 20 NaHCO3, bubbled with 95% O2-5% CO2 (pH 7.4). The tendons of the muscles were tied to a force transducer (400A, Aurora Scientific) and an adjustable hook using nylon sutures. The muscles were immersed in a stimulation chamber containing the Krebs solution continuously bubbled (O_2 95/ Co_2 5%) (at 28°C). The muscle was stimulated to contract using an electrical field between two platinum electrodes (Aurora Scientific 1200A - in vitro System).

The muscle length (Lo) was first adjusted to yield the maximum force. The force–frequency relationships were determined by triggering contraction using incremental stimulation frequencies (0.5 ms pulses at 10–120 Hz for 350 ms at supra- threshold current). Between stimulations the muscle was allowed to rest for ~1 min. Fatigability of the muscles was assessed by measuring the loss of

force in response to repeated stimuli (30 Hz, 300 ms duration) at 1Hz over 10 min. After the measurements of contractile properties were completed, muscles were measured at Lo, dried to remove the buffer, and weighed. The muscle cross-sectional area was determined by dividing muscle weight by its length and tissue density (1.056 g/cm3). Force production was then normalized to the muscle cross-sectional area to determine the specific force.

Muscle Histomorphometry

For mitochondria histomorphometry, EDL and soleus muscles were fixed in 4% PFA/2% glutaraldehyde/0.1M sodium cacodylate pH 7.3, post-fixed in 1% osmium tetraoxide and embedded in epoxy resin (Epon). Ultrathin sections (80 nm) were stained with aqueous uranyl acetate and lead citrate and examined with a JEOL 2000FX transmission electron microscope. For the determination of the cross-section area of muscle fibers, gastrocnemius muscle was fixed in 10% neutral formalin, embedded in paraffin and sectioned at 5μm. Sections were stained with hematoxylin and eosin and analyzed using the ImageJ software. For determination of muscle fiber type composition, gastrocnemius muscle was frozen in liquid N_2-cooled methylbutane. Samples were sectioned at 10μm. SDH, ATPase and COX activity assays were performed as described (Quiat et al., 2011). Images were analyzed using the ImageJ software.

RNASeq

RNA was extracted from each group using RNAqueous®-Micro Total RNA Isolation Kit (ThermoSci, #AM1931) and the quality of purified RNA samples was determined using a Bioanalyzer 2100 (Agilent) with an RNA Pico kit. Extracted

RNA samples were amplified by Ovation® RNA-Seq System V2 (NuGEN) Kit. Amplified cDNA was labeled with Encore biotin module Kit (NuGEN) for RNASeq applications Illumina Truseq RNA Sample Prep v2 using the LT protocol. RNA was sequenced at 30M paired 100 bp reads reads per sample on an Illumina 2500 HISeq instrument.

Bases were called with Illumina's Real Time Analysis (RTA 1.9) (Illumina, 2015b). Adaptors were trimmed and reads were converted from BCL to Fasta format with bcl2fastq 1.8.4 (Illumina, 2015a). Reads were mapped to the mm9 mouse genome with Bowtie2 (Langmead and Salzberg, 2012) 2.0.0-beta7 and TopHat2 (Kim et al., 2013) 2.0.4. Reads were counted with HTSeq-0.6.1p2 (Anders et al., 2015). These data were deposited in the Gene Expression Omnibus (GEO) (Barrett et al., 2013), Accession number, GSE75919.

Experiments were normalized with TMM (Robinson and Oshlack, 2010). Differential expression was estimated using Limma-Voom with weights (Law et al., 2014; Liu et al., 2015). All of the Benjamini-Hochberg (Benjamini and Hochberg, 1995) False discovery rates (fdr) were > 0.90. However, spot checking key genes by PCR, shows that an uncorrected $p \leq 0.02$ is a reliable significance cutoff for this RNASeq experiment. 242 genes were statistically significantly differentially expressed by this cutoff.

To visualize the effect of osteocalcin signaling in myofibers on gene expression independently of the magnitude of expression of each gene, raw counts for a gene were divided by the total number of counts for that gene across samples, and then $\log_2$ transformed. In addition, clustering of all genes which were

differentially expressed with p≤0.02 and range(log_2(normalized-counts)) ≥ 1 (46 genes) was performed (Figure 5A). Clustering was performed with Cluster 3.0 (de Hoon et al., 2004; Eisen et al., 1998). The expression of each gene, and then samples, were mean centered. Both genes and samples were clustered using average-linkage clustering (Everitt et al., 2011). The heatmaps were displayed with JavaTreeView (Saldanha, 2004).

Statistics

All data are presented as mean ± standard error of mean. Statistical analyses were performed using unpaired, two-tailed Student's t test for comparison between two groups and ANOVA test for experiments involving more than two groups. For all experiments, * denotes P ≤ 0.05, ** P ≤ 0.005.

Supplemental References

Anders, S., Pyl, P.T., and Huber, W. (2015). HTSeq--a Python framework to work with high-throughput sequencing data. Bioinformatics *31*, 166-169.

Barrett, T., Wilhite, S.E., Ledoux, P., Evangelista, C., Kim, I.F., Tomashevsky, M., Marshall, K.A., Phillippy, K.H., Sherman, P.M., Holko, M.*, et al.* (2013). NCBI GEO: archive for functional genomics data sets--update. Nucleic Acids Res *41*, D991-995.

Benjamini, Y., and Hochberg, Y. (1995). Controlling the false discovery rate; A practical and powerful approach to multiple testing. J Roy Stat Soc Ser B *57*, 289-300.

Bruning, J.C., Michael, M.D., Winnay, J.N., Hayashi, T., Horsch, D., Accili, D., Goodyear, L.J., and Kahn, C.R. (1998). A muscle-specific insulin receptor knockout exhibits features of the metabolic syndrome of NIDDM without altering glucose tolerance. Mol Cell *2*, 559-569.

de Hoon, M.J., Imoto, S., Nolan, J., and Miyano, S. (2004). Open source clustering software. Bioinformatics *20*, 1453-1454.

Eisen, M.B., Spellman, P.T., Brown, P.O., and Botstein, D. (1998). Cluster analysis and display of genome-wide expression patterns. Proc Natl Acad Sci USA *95*, 14863-14868.

Everitt, B.S., Landau, S., and Leese, M. (2011). Cluster Analysis (Wiley).

Howlett, K.F., Andrikopoulos, S., Proietto, J., and Hargreaves, M. (2013). Exercise-induced muscle glucose uptake in mice with graded, muscle-specific GLUT-4 deletion. Physiol Rep *1*, e00065.

Illumina (2015a). bcl2fastq Conversion Software (Illumina).

Illumina (2015b). Real Time Analysis (RTA).

Kim, D., Pertea, G., Trapnell, C., Pimentel, H., Kelley, R., and Salzberg, S.L. (2013). TopHat2: accurate alignment of transcriptomes in the presence of insertions, deletions and gene fusions. Genome Biol *14*, R36.

Kombu, R.S., Brunengraber, H., and Puchowicz, M.A. (2011). Analysis of the citric acid cycle intermediates using gas chromatography-mass spectrometry. Methods Mol Biol *708*, 147-157.

Krug, S., Kastenmuller, G., Stuckler, F., Rist, M.J., Skurk, T., Sailer, M., Raffler, J., Romisch-Margl, W., Adamski, J., Prehn, C.*, et al.* (2012). The dynamic range of the human metabolome revealed by challenges. FASEB J *26*, 2607-2619.

Langmead, B., and Salzberg, S.L. (2012). Fast gapped-read alignment with Bowtie 2. Nat Methods *9*, 357-359.

Law, C.W., Chen, Y., Shi, W., and Smyth, G.K. (2014). voom: Precision weights unlock linear model analysis tools for RNA-seq read counts. Genome Biol *15*, R29.

Liu, R., Holik, A.Z., Su, S., Jansz, N., Chen, K., Leong, H.S., Blewitt, M.E., Asselin-Labat, M.L., Smyth, G.K., and Ritchie, M.E. (2015). Why weight? Modelling sample and observational level variability improves power in RNA-seq analyses. Nucleic Acids Res *43*, e97.

Qiu, Y., Cai, G., Zhou, B., Li, D., Zhao, A., Xie, G., Li, H., Cai, S., Xie, D., Huang, C.*, et al.* (2014). A distinct metabolic signature of human colorectal cancer with prognostic potential. Clin Cancer Res *20*, 2136-2146.

Quiat, D., Voelker, K.A., Pei, J., Grishin, N.V., Grange, R.W., Bassel-Duby, R., and Olson, E.N. (2011). Concerted regulation of myofiber-specific gene expression and muscle performance by the transcriptional repressor Sox6. Proc Natl Acad Sci U S A *108*, 10196-10201.
Robinson, M.D., and Oshlack, A. (2010). A scaling normalization method for differential expression analysis of RNA-seq data. Genome Biol *11*, R25.
Saldanha, A.J. (2004). Java Treeview--extensible visualization of microarray data. Bioinformatics *20*, 3246-3248.
Serasinghe, M.N., Wieder, S.Y., Renault, T.T., Elkholi, R., Asciolla, J.J., Yao, J.L., Jabado, O., Hoehn, K., Kageyama, Y., Sesaki, H.*, et al.* (2015). Mitochondrial Division Is Requisite to RAS-Induced Transformation and Targeted by Oncogenic MAPK Pathway Inhibitors. Mol Cell *57*, 521-536.
Wang-Sattler, R., Yu, Z., Herder, C., Messias, A.C., Floegel, A., He, Y., Heim, K., Campillos, M., Holzapfel, C., Thorand, B.*, et al.* (2012). Novel biomarkers for pre-diabetes identified by metabolomics. Mol Syst Biol *8*, 615.
Zeigerer, A., Lampson, M.A., Karylowski, O., Sabatini, D.D., Adesnik, M., Ren, M., and McGraw, T.E. (2002). GLUT4 retention in adipocytes requires two intracellular insulin-regulated transport steps. Mol Biol Cell *13*, 2421-2435.
Zhang, Y., Zhang, S., Marin-Valencia, I., and Puchowicz, M.A. (2015). Decreased carbon shunting from glucose toward oxidative metabolism in diet-induced ketotic rat brain. J Neurochem *132*, 301-312.